TABLE 1. *Maeda's questionnaire for Type A behavior pattern*

Questions	Always	Occasionally	Hardly
1. Do you have a busy daily life?			
2. Do you feel being pressed for time in your daily life?			
3. Do you easily become enthusiastic over your job or other things?			
4. When you are absorbed in your job, do you find it difficult to change your mind?			
5. Are you a perfectionist?			
6. Do you have confidence in yourself?			
7. Do you easily feel tense?			
8. Do you easily feel irritated or angry?			
9. Are you punctual with everything?			
10. Are you unyielding?			
11. Do you have an intense temper?			
12. Do you easily become competitive about job or other things?			

Each question had three responses. Points 2, 1, and 0 were given to the answers of "always", "occasionally", and "hardly" for 1, 2, 3, 4, 7, 8, 10, 11 and 12 nine questions, and the points were doubled for 5, 6 and 9 three questions. A total score of 17 or greater was defined as type A.

determines volume pulse form. Volume waveforms were stored for a sampling time of 10 s with automatic gain analysis and quality adjustment. This instrument simultaneously records the baPWV on the left and right sides. The highest baPWV on both sides was determined, and subsequent statistical analyses were performed using these values (Liu et al. 2005; Tomiyama et al. 2005).

Statistical analysis

Data are expressed as mean ± S.D. All statistical analyses were performed using StatView-5 software (SAS Institute Inc., Cary, NC, USA). Student's *t*-test was used to examine statistical difference of baPWV, BMI or SBP between subjects with Type A behavior and subjects without Type A behavior. Multiple linear regression analysis was performed to evaluate the association between baPWV and age, BMI, SBP, DBP, and Type A Scale in the subjects. Pearson's correlation coefficient analysis was used to assess the relation between baPWV and SBP in subjects with Type A behavior and subjects without Type A behavior and the relation between PWV and Type A Scale in 307 subjects. Partial correlation coefficient analysis was used to describe the correlation between baPWV and age using SBP as covariate. $p < 0.05$ was regarded as statistically significant.

RESULTS

Comparison of baPWV, BMI, and SBP between the Type A group and the non-Type A group

The subjects' characteristics are summarized in Table 2. Three hundreds and seven normal Japanese subjects were classified into either the Type A group ($n = 90$) or the non-Type A group ($n = 217$). BaPWV in the Type A group was significantly higher than that in non-Type A group. SBP and BMI were also significantly higher in the Type A group than those in the non-Type A group.

TABLE 2. *Characteristics of subjects*

Variables	Type A group	Non-Type A group
n	90	217
Age (years)	34.29 ± 16.54	33.92 ± 14.94
BMI (kg/m^2)	21.96 ± 2.94	21.24 ± 2.49*
BaPWV (m/sec)	11.88 ± 2.35	10.96 ± 1.25*
SBP (mmHg)	124.94 ± 8.24	122.27 ± 9.14*

Data represent mean ± S.D.
* $p < 0.05$ (Student's *t*-test).

Correlation of baPWV with age and SBP in the Type A group and in the non-Type A group

Table 3 shows the results of multiple regression analysis including baPWV and age, BMI, SBP, DBP, or Type A Scale. Age, SBP, and Type A Scale were significantly associated with baPWV, whereas BMI and DBP showed no significant association.

TABLE 3. *Multiple regression analysis of the factors associated with baPWV*

Variables	β	p value
Age	0.57	0.001
BMI	0.01	0.895
SBP	0.14	0.012
DBP	0.08	0.102
Type A Scale	0.29	0.001

After adjusting for SBP, baPWV showed a significant positive partial correlation with age both in the Type A group ($r = 0.72$, $p < 0.05$) (Fig. 1A) and in the non-Type A group ($r = 0.54$, $p < 0.05$) (Fig. 1B). Comparisons between straight-line regression slopes were made using an analysis of covariance. The slope of baPWV vs age in the Type A group ($Y = 7.946 + 0.102X$) was significantly larger than that in the non-Type A group ($Y = 10.251 + 0.044X$) ($F = 45.38$, $p < 0.001$).

BaPWV showed a significant positive correlation with SBP both in the Type A group ($r = 0.41$, $p < 0.05$) (Fig. 2A) and in the non-Type A group ($r = 0.31$, $p < 0.05$) (Fig. 2B). The slope of baPWV vs SBP in the Type A group ($Y = -2.831 + 0.118X$) was significantly larger than that in the non-Type A group ($Y = 5.816 + 0.042X$) ($F = 10.99$, $p < 0.001$).

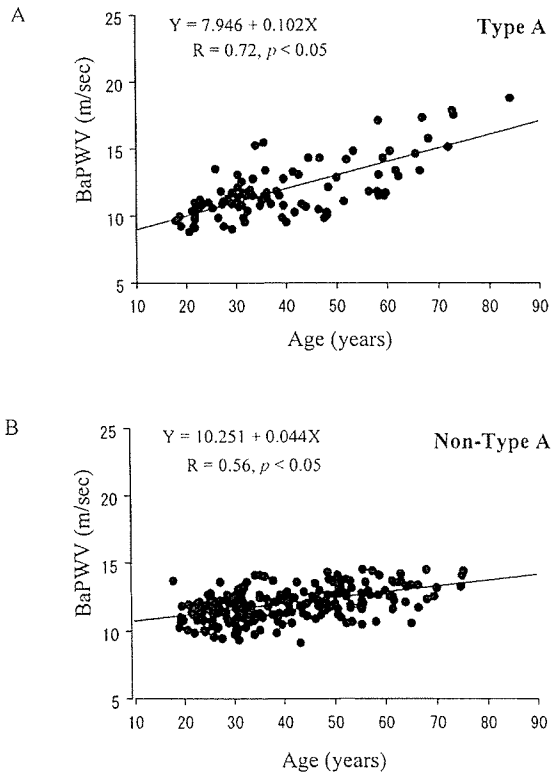

Fig. 1. Relations between baPWV and age adjusted for SBP in Type A group (A) and non-Type A group (B).

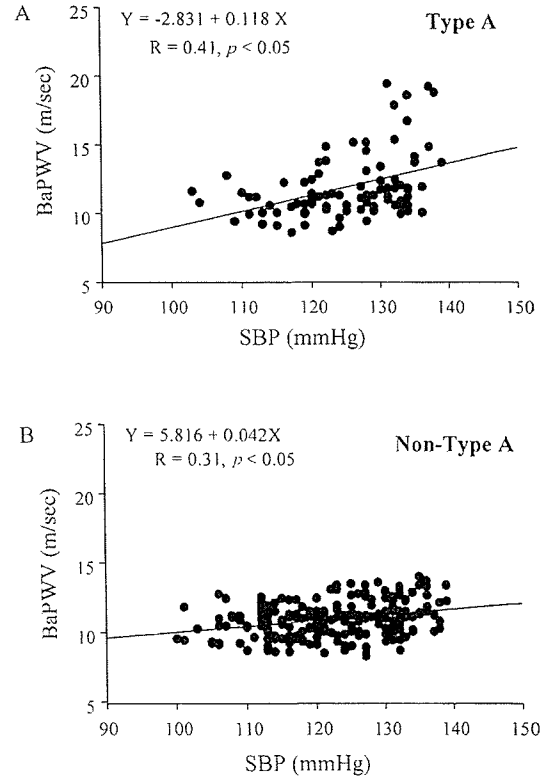

Fig. 2. Relations between baPWV and SBP in the Type A group (A) and in the non-Type A group (B).

Correlation of baPWV and SBP with the Type A Scale in 307 subjects

BaPWV showed a significant positive correlation with the Type A Scale in 307 subjects (r = 0.34, $p < 0.05$) (Fig. 3A). However, SBP showed no significant correlation with the Type A Scale (Fig. 3B).

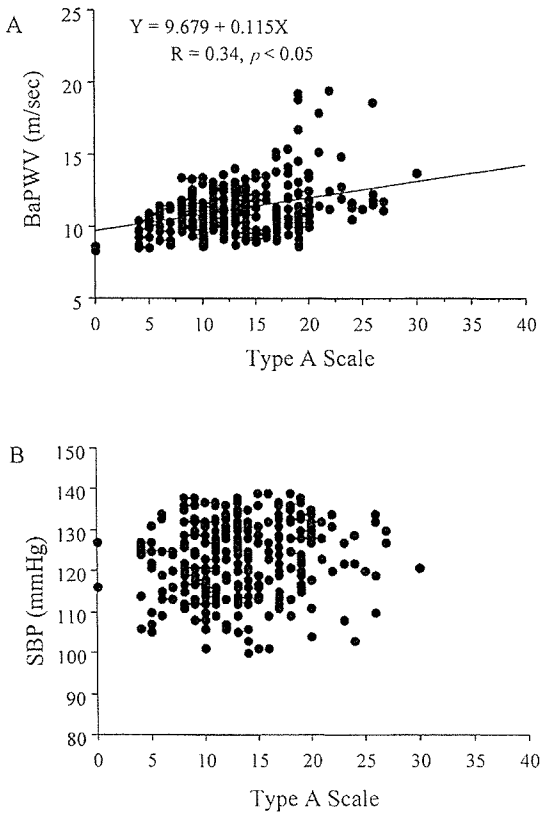

Fig. 3. Relations between baPWV and Type A Scale in 307 subjects (A) and Relations between SBP and Type A Scale in 307 subjects (B).

Discussion

In the present study, we compared the baPWV of subjects with Type A behavior and those without Type A behavior for the first time. Our major finding is that the baPWV of the Type A group had higher values than those of the non-Type A group. Therefore, our results suggest that subjects expressing the Type A behavior pattern have a higher risk for arteriosclerotic diseases than do subjects showing a non-Type A behavior pattern.

Arterial stiffness is a cause of premature return of reflected waves in late systole, increasing central pulse pressure and the load on the ventricle, reducing ejection fraction, and increasing myocardial oxygen demand (Laurent et al. 2001). The principal outcomes of these changes are left ventricular hypertrophy, aggravation of coronary ischemia, and increased fatigue of arterial wall tissues (Shoji et al. 2001; Blacher et al. 2003). Higher systolic blood pressure and pulse pressure, lower diastolic blood pressure, and left ventricular hypertrophy have been identified as independent factors of cardiovascular morbidity. Arterial stiffness is correlated with atherosclerosis, probably through the effects of cyclic stress on arterial wall thickening (Laurent et al. 2001).

The synergistic effect of hypertension and arteriosclerosis may appear as a higher PWV value. The degree of PWV elevation may correspond to the degree of arteriosclerotic change: a very high PWV may indicate that the arteriosclerotic process is already well established (Ogawa et al. 2003; Yokoyama et al. 2003). Thus, an increased PWV was associated with arteriosclerotic risk factors (Altun et al. 2004; Fujiwara et al. 2004; Tomiyama et al. 2004).

We also examined the correlation between baPWV and age. BaPWV showed a significantly positive correlation with age in subjects both with Type A behavior and in subjects without Type A behavior. The significant positive correlation found between baPWV and age showed that arteries become less elastic with age, and arterial stiffening was observed with increasing age (Oren et al. 2003). Aging induces structural and functional abnormalities such as arterial wall hypertrophy and degeneration or disorganization of the medial layer. These changes increase PWV because of increased arterial stiffness (Tomiyama et al. 2004, 2005).

Moreover, we found that the straight-line regression slope of baPWV vs age was significantly larger in subjects with Type A behavior than in subjects without Type A behavior. These results suggest that the increase of baPWV with age occurred earlier, the development of arterio-

sclerosis was faster, and an overall higher cardiovascular risk was shown in subjects expressing Type A behavior than in subjects not expressing Type A behavior. This trend may be associated with the effects on psychosocial variables of the Type A behavior pattern. A series of recent findings support adverse psychosocial effects relevant to arteriosclerosis under conditions of mental stress. Psychological variables may also impact the course of coronary disease through behavioral mechanisms (Rutledge et al. 2001).

Type A men, irrespective of coronary status, showed larger systolic and diastolic blood pressure response to both mental and physical stress than did Type B men (Sundin et al. 1995). Type A behavior may produce mental overload and stress, while coronary-prone exhaustion is characterized by inappropriate coping with environmental stress and giving up when confronted with life distress. Type A behavior is seen as personality traits, but it may also be a set of reactions to environmental stress and thus easily influenced by life events and working stress (Keltikangas-Jarvinen et al. 1996). Recently, it was reported that there exists a certain relationship between psychological factors and the extent of atherosclerosis measured by coronary angiography (Whiteman et al. 2000). There are few studies investigating the psychosocial factors related to these measures of arteriosclerotic disease processes. Psychosocial factors have been shown to contribute significantly to the development and clinical manifestations of coronary artery disease (CAD) (Whiteman et al. 2000). Type A behavior pattern is predictive of increased risk of coronary arteriosclerosis and might contribute to premature coronary arteriosclerosis and increased risk for CAD (Donker 2000; Yoshimasu et al. 2000, 2001; Sparagon et al. 2001).

Heart rate, lipid profiles and plasma glucose also influence PWV. However, these parameters were not examined in this study. It might be of interest to examine whether Type A behavior influences them.

In summary, the baPWV in the Type A group was significantly higher than that observed in the non-Type A group. The baPWV showed a positive correlation with age both in the Type A and the non-Type A groups. Moreover, the increasing trend of baPWV against age seen in the Type A group had a larger value than that of non-Type A group. Our results suggest that arteriosclerosis might be promoted earlier in subjects showing the Type A behavior pattern. Type A behavior pattern is confirmed as a risk factor for arteriosclerosis, and may promote to increase the risk of the cardiovascular disease related to arteriosclerosis. These findings may be associated with the differences in their psychosocial factors.

Acknowledgments

This work was partly supported by a Grant-in-aid for Scientific Research (11480253), a Research Grant for Cardiovascular Diseases from the Ministry of Health and Welfare and Program for Promotion of Fundamental Studies in Health Science of Organizing for Drug ADR Relief, R&D Promotion and Product Review of Japan, and Health and Labour Sciences Research Grants for Research on Advanced Medical Technology.

References

Altun, A., Erdogan, O. & Yildiz, M. (2004) Acute effect of DDD versus VVI pacing on arterial distensibility. *Cardiology*, **102**, 89-92.

Blacher, J., Safar, M.E., Guerin, A.P., Pannier, B., Marchais, S.J. & London, G.M. (2003) Aortic pulse wave velocity index and mortality in end-stage renal disease. *Kidney Int.*, **63**, 1852-1860.

Buller, J.C., Kritz-Silverstein, D., Barrett-Connor, E. & Wingard, D. (1998) Type A behavior pattern, heart disease risk factors, and estrogen replacement therapy in postmenopausal women: the Rancho Bernardo Study. *J. Womens Health*, **7**, 49-56.

Donker, F.J. (2000) Cardiac rehabilitation: a review of current developments. *Clin. Psychol. Rev.*, **20**, 923-943.

Fujiwara, T., Saitoh, S., Takagi, S., Ohnishi, H., Ohata, J., Takeuchi, H., Isobe, T., Chiba, Y., Katoh, N., Akasaka, H. & Shimamoto, K. (2004) Prevalence of asymptomatic arteriosclerosis obliterans and its relationship with risk factors in inhabitants of rural communities in Japan: Tanno-Sobetsu study. *Atherosclerosis*, **177**, 83-88.

Gallacher, J.E., Sweetnam, P.M., Yarnell, J.W., Elwood, P.C. & Stansfeld, S.A. (2003) Is type A behavior really a trigger for coronary heart disease events? *Psychosom. Med.*, **65**, 339-346.

Keltikangas-Jarvinen, L., Raikkonen, K., Hautanen, A. & Adlercreutz, H. (1996) Vital exhaustion, anger expression, and pituitary and adrenocortical hormones. Implications for the insulin resistance syndrome. *Arterioscler Thromb Vasc. Biol.*, **16**, 275-280.

Laurent, S., Boutouyrie, P., Asmar, R., Gautier, I., Laloux, B., Guize, L., Ducimetiere, P. & Benetos, A. (2001) Aortic stiffness is an independent predictor of all-cause and cardiovascular mortality in hypertensive patients. *Hyperten-*

sion, **37**, 1236-1241.

Liu, H., Yambe, T., Zhang, X., Saijo, Y., Shiraishi, Y., Sekine, K., Maruyama, M., Kovalev, Y.A., Milyagina, I.A., Milyagin, V.A. & Nitta, S. (2005) Comparison of brachial-ankle pulse wave velocity in Japanese and Russians. *Tohoku J. Exp. Med.*, **207**, 263-270.

Maeda, S. (1991) Application of a brief questionnaire for the behavior pattern survey. *Type A*, **2**, 33-40.

Ogawa, O., Onuma, T., Kubo, S., Mitsuhashi, N., Muramatsu, C. & Kawamori, R. (2003) Brachial-ankle pulse wave velocity and symptomatic cerebral infarction in patients with type 2 diabetes: a cross-sectional study. *Cardiovasc. Diabetol.*, **2**, 10.

Ogawa, O., Hayashi, C., Nakaniwa, T., Tanaka, Y. & Kawamori, R. (2005) Arterial stiffness is associated with diabetic retinopathy in type 2 diabetes. *Diabetes Res. Clin. Pract.*, **68**, 162-166.

Oren, A., Vos, L.E., Bos, W.J., Safar, M.E., Uiterwaal, C.S., Gorissen, W.H., Grobbee, D.E. & Bots, M.L. (2003) Gestational age and birth weight in relation to aortic stiffness in healthy young adults: two separate mechanisms? *Am. J. Hypertens.*, **16**, 76-79.

Rutledge, T., Reis, S.E., Olson, M., Owens, J., Kelsey, S.F., Pepine, C.J., Reichek, N., Rogers, W.J., Merz, C.N., Sopko, G., Cornell, C.E. & Matthews, K.A. (2001) Psychosocial variables are associated with atherosclerosis risk factors among women with chest pain: the WISE study. *Psychosom. Med.*, **63**, 282-288.

Shoji, T., Emoto, M., Shinohara, K., Kakiya, R., Tsujimoto, Y., Kishimoto, H., Ishimura, E., Tabata, T. & Nishizawa, Y. (2001) Diabetes mellitus, aortic stiffness, and cardiovascular mortality in end-stage renal disease. *J. Am. Soc. Nephrol.*, **12**, 2117-2124.

Sparagon, B., Friedman, M., Breall, W.S., Goodwin, M.L., Fleischmann, N. & Ghandour, G. (2001) Type A behavior and coronary atherosclerosis. *Atherosclerosis*, **156**, 145-149.

Sundin, O., Ohman, A., Palm, T. & Strom, G. (1995) Cardiovascular reactivity, Type A behavior, and coronary heart disease: comparisons between myocardial infarction patients and controls during laboratory-induced stress. *Psychophysiology*, **32**, 28-35.

Tomiyama, H., Arai, T., Koji, Y., Yambe, M., Hirayama, Y., Yamamoto, Y. & Yamashina, A. (2004) The relationship between high-sensitive C-reactive protein and pulse wave velocity in healthy Japanese men. *Atherosclerosis*, **174**, 373-377.

Tomiyama, H., Koji, Y., Yambe, M., Shiina, K., Motobe, K., Yamada, J., Shido, N., Tanaka, N., Chikamori, T. & Yamashina, A. (2005) Brachial - ankle pulse wave velocity is a simple and independent predictor of prognosis in patients with acute coronary syndrome. *Circ. J.*, **69**, 815-822.

Watanabe, I., Tani, S., Anazawa, T., Kushiro, T. & Kanmatsuse, K. (2005) Effect of pioglitazone on arteriosclerosis in comparison with that of glibenclamide. *Diabetes. Res. Clin. Pract.*, **68**, 104-110.

Whiteman, M.C., Deary, I.J. & Fowkes, F.G. (2000) Personality and social predictors of atherosclerotic progression: Edinburgh Artery Study. *Psychosom. Med.*, **62**, 703-714.

Woodside, J.V., Mcmahon, R., Gallagher, A.M., Cran, G.W., Boreham, C.A., Murray, L.J., Strain, J.J., Mcnulty, H., Robson, P.J., Brown, K.S., Whitehead, A.S., Savage, M. & Young, I.S. (2004) Total homocysteine is not a determinant of arterial pulse wave velocity in young healthy adults. *Atherosclerosis*, **177**, 337-344.

Yamashina, A., Tomiyama, H., Arai, T., Hirose, K., Koji, Y., Hirayama, Y., Yamamoto, Y. & Hori, S. (2003) Brachial-ankle pulse wave velocity as a marker of atherosclerotic vascular damage and cardiovascular risk. *Hypertens. Res.*, **26**, 615-622.

Yokoyama, H., Shoji, T., Kimoto, E., Shinohara, K., Tanaka, S., Koyama, H., Emoto, M. & Nishizawa, Y. (2003) Pulse wave velocity in lower-limb arteries among diabetic patients with peripheral arterial disease. *J. Atheroscler. Thromb.*, **10**, 253-258.

Yoshimasu, K., Liu, Y., Kodama, H., Sasazuki, S., Washio, M., Tanaka, K., Tokunaga, S., Kono, S., Arai, H., Koyanagi, S., Hiyamuta, K., Doi, Y., Kawano, T., Nakagaki, O., Takada, K., Nii, T., Shirai, K., Ideishi, M., Arakawa, K., Mohri, M. & Takeshita, A. (2000) Job strain, Type A behavior pattern, and the prevalence of coronary atherosclerosis in Japanese working men. *J. Psychosom. Res.*, **49**, 77-83.

Yoshimasu, K. (2001) Relation of type A behavior pattern and job-related psychosocial factors to nonfatal myocardial infarction: a case-control study of Japanese male workers and women. *Psychosom. Med.*, **63**, 797-804.

IFMBE Proceedings Volume 14, 2006
World Congress on Medical Physics and Biomedical Engineering (ISBN: 3-540-36839-6)

Evaluation of Cardiac Function of the Patients with Left Ventricular Assist Device by Transesophageal Echocardiography

Y. Saijo[1], Y. Saiki[2], A. Iguchi[2], K. Tabayashi[2], Y. Shiraishi[1], K. Sekine[1] and T. Yambe[1]

[1] Department of Medical Engineering and Cardiology, Institute of Development, Aging and Cancer, Tohoku University, Sendai, Japan
[2] Department of Cardiovascular Surgery, Tohoku University Hospital, Sendai, Japan

Abstract— **The control of left ventricular assist device (LVAD) has been based on pressures of left ventricle (LV), aorta (AO) and pulmonary artery (PA) and flows in AO and PA. These parameters are one-dimensional and suitable for control of LVAD because they are numerical and quantitative. However, evaluation of the cardiac function by echocardiography is very useful in clinical settings because the cardiac function changes rapidly and dramatically. Transesophageal echocardiography is very useful for the assessment of cardiac function of the patients with LVAD implantation because it can detect and visualize what is happening in the heart immediately and directly.**

Keywords— **Transesophageal echocardiography, cardiac function, left ventricular assist device,**

I. Introduction

The control of left ventricular assist device (LVAD) has been based on pressures of left ventricle (LV), aorta (AO) and pulmonary artery (PA) and flows in AO and PA. These parameters are one-dimensional and suitable for control of LVAD because they are numerical and quantitative. However, evaluation of the cardiac function by echocardiography is very useful in clinical settings because the cardiac function changes rapidly and dramatically. For example, slight dilatation of LV may lead to large a mitral regurgitation due to tethering effect when the cardiac function is deteriorated and LV was enlarged.

The objectives of the present study are to observe LV volume and regurgitations and to evaluate cardiac function of the patients with LVAD by transesophageal echocardiography.

II. Methods

A. Patients and Methods

522 consecutive cases of cardiovascular surgery were evaluated by intra-operative transesophageal echocardiography to assess cardiac function. The observation period is from May 2000 to April 2006. The transesophageal ultrasound probe (Omniplane II, Philips, Andover, USA) was inserted after induction of general anesthesia. The ultrasound device was SONOS 5500 (Philips, Andover, USA). The ejection fraction (EF) obtained with area-length method, assessment of grades of mitral, aortic and tricuspid valvular regurgitation, and dimensions of the aortic root were recorded. Among these cases, LVAD was implanted for 5 patients. In these 5 patients, right ventricular (RV) wall motion and RV volume were also measured.

The images and movies were recorded on a digital video recorder (DCR-TRV30, Sony, Tokyo, Japan). Images and movies were captured via IEEE1394 to a personal computer (VAIO-RZ 55, Sony, Tokyo, Japan) for further evaluation.

III. Results

The condition of anesthesia, drug administration and volume infusion lead to LV enlargement. In some cases, mild mitral regurgitation (MR) worsened to severe MR.

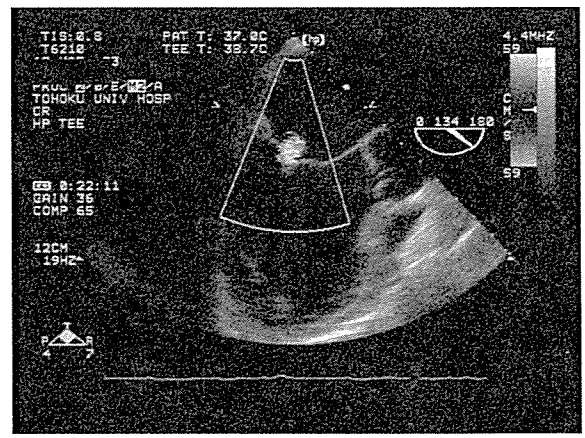

Fig. 1 Mild mitral regurgitation (MR) after induction of general anesthesia.

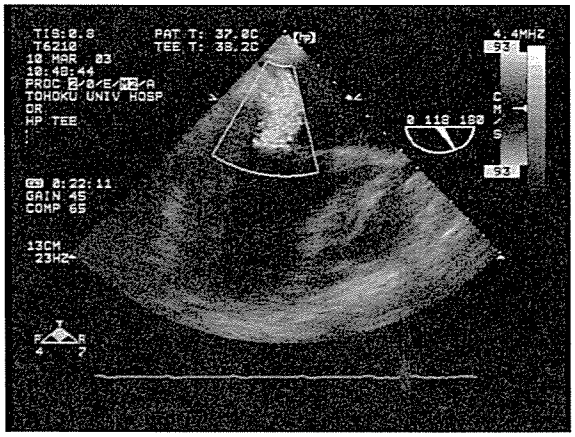

Fig. 2 Worsening of MR after infusion of volume.

We also experienced a case with severe "To and fro" tricuspid regurgitation without turbulent flow by rapid volume infusion.

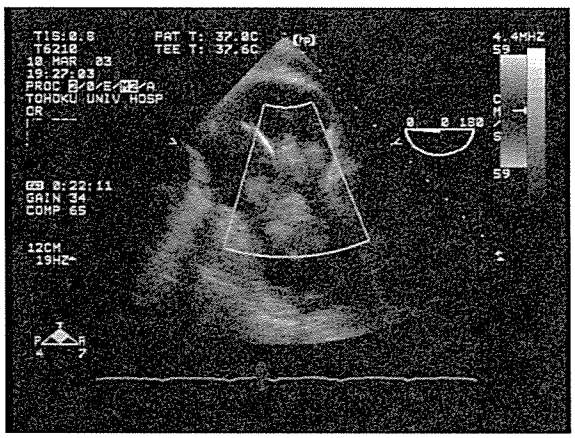

Fig. 3 Tricuspid regurgitation (TR) without turbulent flow

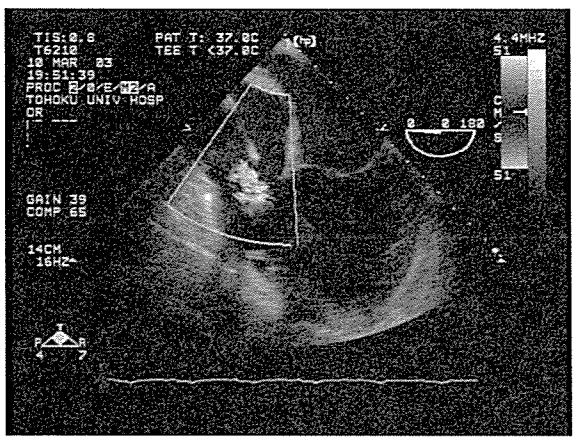

Fig. 4 Return to the mild TR

We also experienced a case with ventricular tachycardia immediately after the surgery was started. In the case, smoke-like-echo in LV was observed unless sufficient PCPS support.

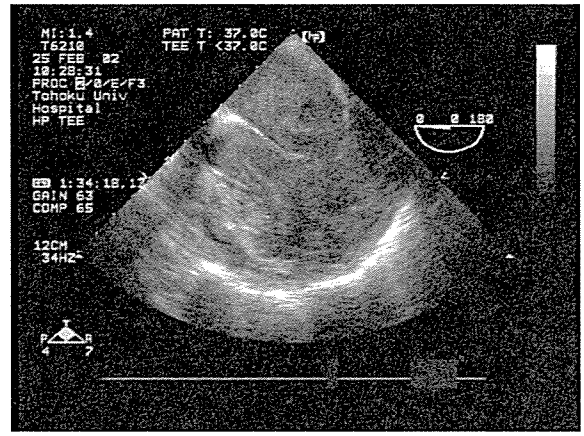

Fig. 5 Smoke-like echo in left atrium and ventricle at ventricular fibrillation

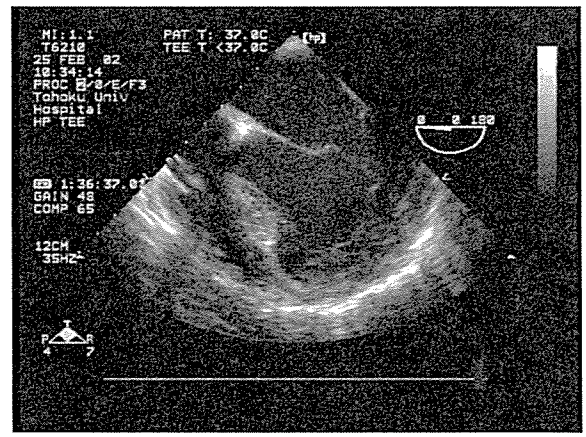

Fig. 6 Smoke-like echo disappeared after returning to sinus rhythm with DC conversion

One case with LVAD implantation showed dramatically improvement of LVEF (from 15% to 60%) at the three month but cardiac output of natural heart was almost zero at that time. One and half year after, the cardiac function was improved and LVAD exchange was operated without cardiopulmonary support.

One case which was successful for LVAD weaning, LV volume was fluctuated by the small difference of natural heart rate and LVAD heart rate.

IV. Conclusions

Transesophageal echocardiography is very useful for the assessment of cardiac function of the patients with LVAD implantation because it can detect and visualize what is happening in the heart immediately and directly.

Author: Yoshifumi Saijo
Institute: Department of Medical Engineering and Cardiology, Institute of Development, Aging and Cancer, Tohoku University
Street: 4-1 Seiryomachi, Aoba-ku
City: Sendai 980-8575
Country: Japan
Email: saijo@idac.tohoku.ac.jp

IFMBE Proceedings Volume 14, 2006
World Congress on Medical Physics and Biomedical Engineering (ISBN: 3-540-36839-6)

An Implantable Probe for Chronic Observation of Microcirculation

Kou Imachi[1], Shuichi Mochizuki[3], Atsushi Baba[4], Takashi Isoyama[5]
Itsuro Saito[6], Koki Takiura[7], Tsuneo Chinzei[6], Yasuyuki Shiraishi[2],
Tomoyuki Yambe[2], and Yusuke Abe[5]

1 TUBERO, Tohoku University, Sendai, Japan
2 IDAC, Tohoku University, Sendai, Japan
3 Department of Biomedical Engineering, Osaka Institute of Technology
4 Saitama Medical College
5 Department of Biomedical Engineering, Graduate School of Medicine, University of Tokyo
6 RCAST, University of Tokyo
7 Faculty of Engineering, Yamagata University

Abstract-- **Whether the pulsatile flow is essential for living body or not is long-term controversial point between circulatory physiologist and artificial heart researchers. Especially, since an axial flow pump, continuous flow pump, has begun to use clinically in 2001, and could keep the patients alive for more than few years, this problem has become to be thought as very important physiological and pathophysiological problem. The objective of this study is to develop an implantable probe to observe microcirculation under artificial circulation.**

The principle of the probe developed in this study is the following; A thin living tissue put directly on a highly integrated CCD(charge coupled device) and illuminated from the backside of the tissue with LED(light emitting diode). The microvascular nets in the tissue will be projected on the CCD surface like a contact photograph, which produces an image on a TV screen. The problems are how to magnify to be able to observe erythrocyte flow, how to control the focus, how to electrically insulate and how to compactmize.

After several method trials to magnify the image, a micro lens having 2 mm in diameter, 2mm long and 6 times magnification, was designed and made with acrylic resin. The lens was installed into a CCD camera with 8 mm in diameter and 60 mm long. The camera could magnify an image about 650 times on a 14 inches TV screen. A clear microcirculation image including capillary flow could be observed when the camera was implanted into the connective tissue under the skin of a rabbit. Now focus control system is developing for the camera to be implanted chronically in animal

Keywords—**Microcirculation, Pulsatility, Continuous flow, CCD(Charge coupled devise), Artificial heart**

I. Introduction

The pulsatility of the circulatory system has been belived to be essential in the living body until Nose, etal had succeeded to survive a calf for 90 days under continuous flow condition with centrifugal blood pump in 1978. Moreover, many kinds of continuous flow ventricular assist devices(VAD), axial flow pump and centrifugal pump, has begun to use clinically as bridge to heart transplantation since 2000. Although many patients implanted continuous flow VAD can survive for more than few years, their flow have pulsatility by their own residual heart beat. So, it is still important controversial point whether the pulsatility is essential or not for the living body to survive normally.

It would be very important to observe micro-circulation for evaluating the necessity of pulsatility. However, there is no way to observe microcirculation chronically without anesthesia in the animal experiment. We have been developing an implantable probe for chronic observation of microcirculation since 1987. In this article, the authors would like to introduce the history and the present status of the probe.

II. Materials and Method[1-4]

A. CCD probe for contact observation of microcirculation

The first idea to develop a probe depended on the following principle. As the integration of the CCD(charge coupled device) has been increasing by the development of micro and nano-technology, it was expected to be observed microcirculation without lens as a contact photograph by direct contacting the living tissue with CCD surface and lighting from the back side of the tissue(Fig. 1). We tried it in acute animal experiment after envelope CCD surface with thin film for the electrical insulation. The micro-vasculature of rat mesentery was projected on TV screen. Then the first probe was developed by the following manner; A 0.5-inch CCD with 250K or 400K pixels was used in this study. Usually, a CCD on the market is packed in a ceramic case that is covered with a glass. The CCD surface level is 1.5 mm under from the edge of the ceramic package after removal of

its cover glass. To ensure a good contact between the tissue and the CCD surface, a fiber optic plate(FOP) which is a integrated hexagonal core glass rod with 2 mm long and could send a image from one end to another without distortion, was attached on the CCD surface. The residual gap in the ceramic package was filled up with room temperature valcanized(RTV) silicone adhesive or epoxy resin, and the outside of the package including leadwires was molded with epoxy resin for the electrical insulation. A LED was fixed at the center of the CCD, 10mm above the FOP with a specially designed microstand. Figure 2 shows the schema of the probe and Fig.3 is the actual probe

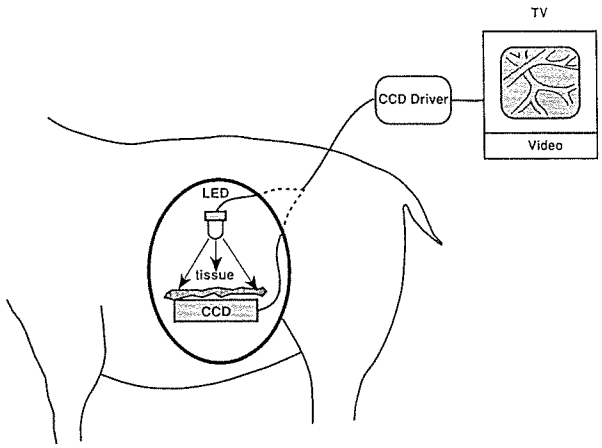

Fig.1 The principle oof implanted probe to observe microcirculation

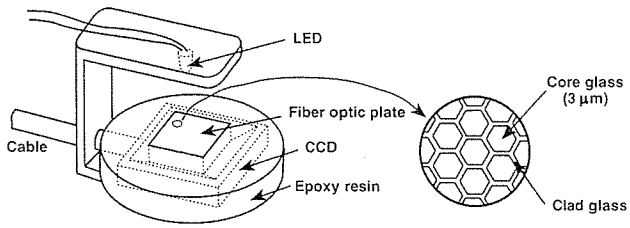

Fig.2 Fabrication of implantable probe using FOP

Fig. 3 First implantable probe with LED

Figure 4 shows a photograph of subcutaneous connective tissue of a rabbit taken by this probe. An arteriole and venule with a diameter as small as 20 – 30 μm could be observed.

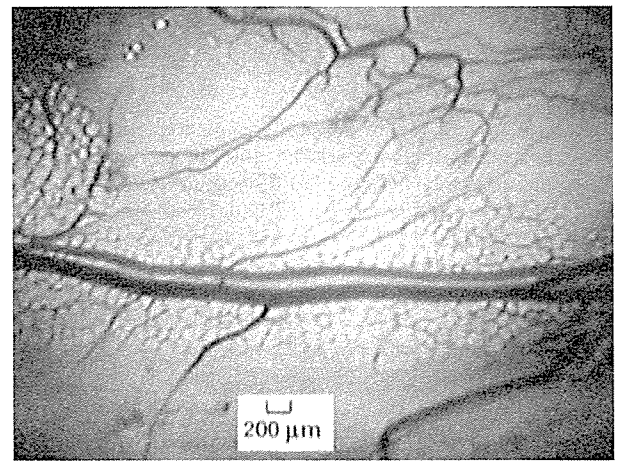

Fig. 4 Microvasculature of connective tissue

To observe the capillary circulation, new probe used tapered FOP with 3 times magnification was designed as Fig,5. A figure on the probe was magnified 165 times on a TV screen with 14 inches. Figure 6 is a photograph of rat mesentery taken by this probe. Capillary vessels could be recognized with ther circulation.

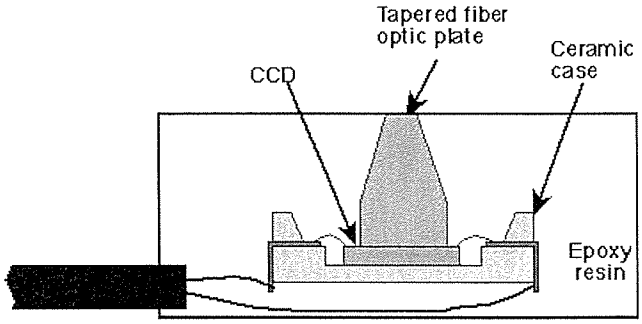

Fig. 5 Probe with a tapered FOP with 3 times magnification

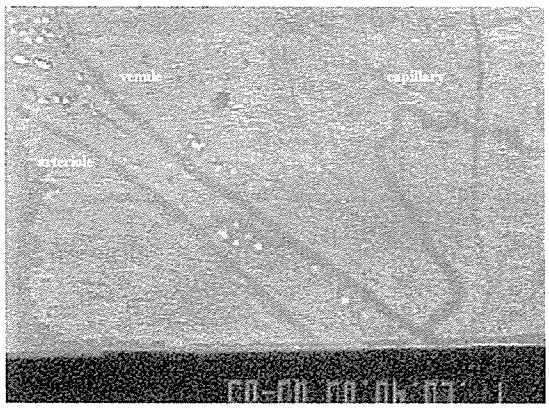

Fig. 6 Microvasculature of rat mesentary

B. Implantable probe with a micr- lens

One of the problems of contact observation probe with FOP was the difficulty to get a fine focused image when the tissue on the stage had some thickness such as omentum and fascia. The fixation method without restriction of the blood flow was another difficulty, especially the animal moves violently, the microcirculatory image became out of focus. So, micro-lens system with focus mechanism was required to develop.

A single micro-lens with 4 mm in diameter and 4.2 mm long was made with acrylic resin. It is aspheric and has 3 times magnification. The lens was fabricated with CCD camera as shown in Fig. 7. The distance between objective and lens, and lens and CCD surface was 3 and 9 mm, respectively. The real magnification on a 14 inch TV screen was 165 times in in-vitro experiment.

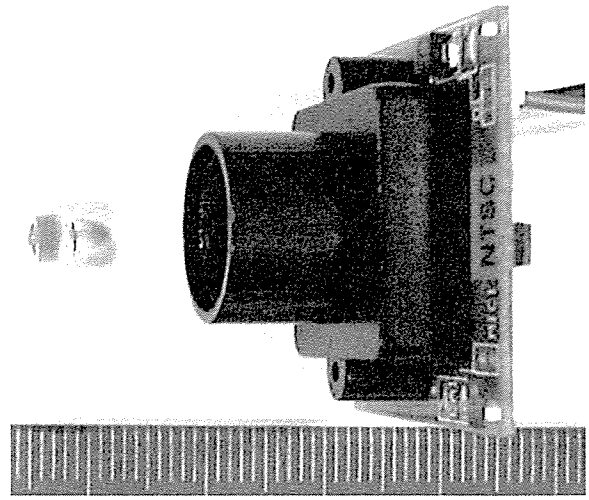

Fig. 7 Micro-lens and CCD camera

Three types of focusing mechanisms, screw type, gear & cam and air bag type, were tried,. Fig. 8 shows the screw type probe in which the focus was adjusted by turning the stage. It was implanted into a goat as shown in Fig. 9. This goat was the first animal observing her own microcirculation. However in this system, the focus couldn't adjust from outside the body after implantation. A gear train focus adjust system(Fig. 10) was difficult to adjust precisely, and the size became big. Air bag type was the best from the view points of accuracy and size. CCD having a driver and micro-lens was packed into a acrylic resin case (37x37x38mm) with a thin transparent stage for putting on a living tissue. An air bag placed at the back side of CCD unit, could inflate and deflate from the out side and change precisely the distance between the lens and stage for focusing between the lens and stage for focusing. Figure 11 shows the probe incorporated an air bag. The probe was implanted into a rabbit and subcutaneous connective tissue and/or fascia was fixed on the stage. A weak light from LED was projected from the backside of the tissue. CCD image was sent to TV by a transmitter fixed on the skin. The flow of erythrocytes and leukocytes in the capillaries as well as in the arteriole and venula could be observed on a TV screen as shown in Fig.12.

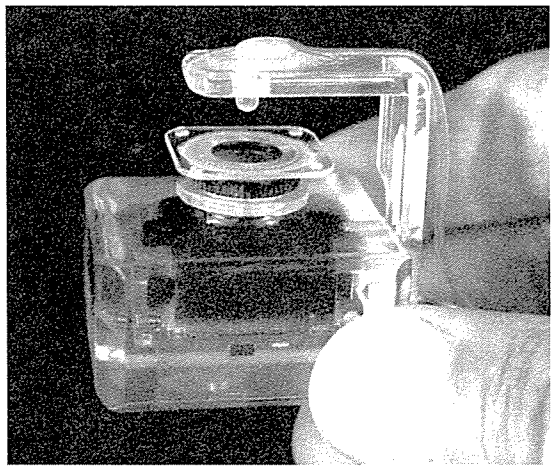

Fig. 8 implantable probe with screw type focus adjust system

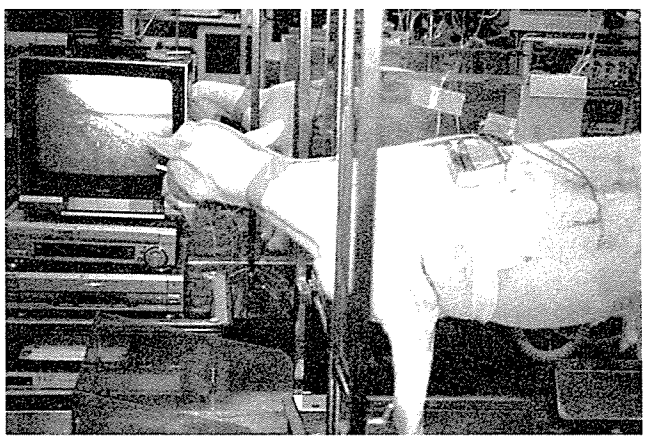

Fig.9 The first goat observed her own microcirculation

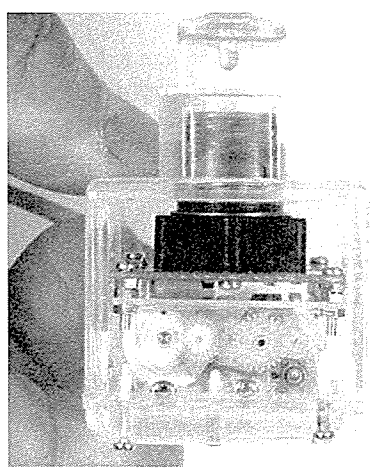

Fig. 10 Gear train forcus adjust system

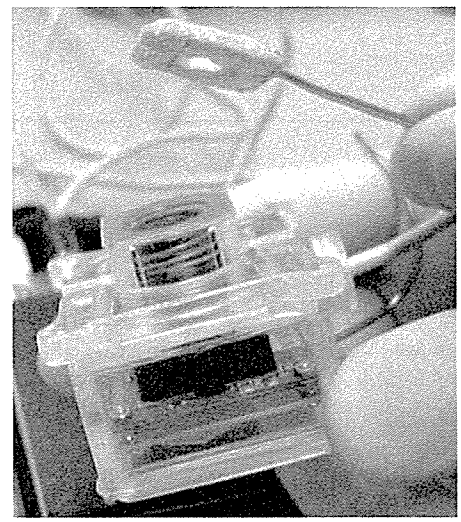

Fig.11 implantable probe with air bag focus adjustsystem

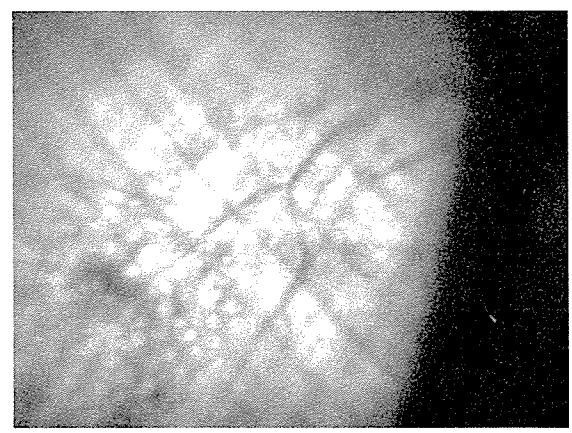

Fig. 12 Microcirculation in the fascia of rabbit

C. Implantable probe with high magnification

Although the last model of implantable probe exhibited to be able to observe capillary flow, the magnification was not enough to analyze erythrocyte speed, etc. And it was preferable to smallen the total size for long-term implantation in the animal. A new probe with high magnification and small size was designed. A micro-lens having 2 mm in diameter, 2 mm long and 6 times magnification was designed and made of acrylic resin. The lens was installed into a CCD camera with 8 mm in diameter and 60 mm long(Fig.13). The probe could magnify the image on the stage about 650 times on a 14 inch TV screen. An acute experiment was performed with a rabbit. A clear microcirculation image including capillary flow could be observed when the camera was inserted into subcutaneous

connective tissue(Fig.14). The flowing erythrocytes were recognized. The probe size became easy to insert into animal.

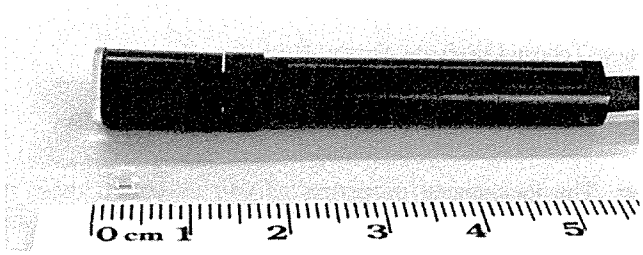

Fig.13 Newly developed micro-lens and probe

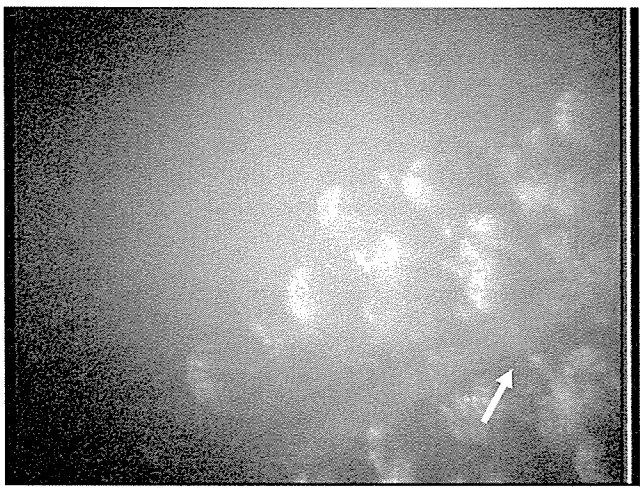

Fig.14 Microvasculature of rabbit subcutaneous connective tissue(arrowshows a capillary vessel)

III. Discussion

It would be very important problem to clarify whether pulsatility of the blood flow is essential for the living body or not, especially to develop future artificial heart. One of the effective method to prove it, is to observe microcirculation chronically and continuously without restriction such as anesthesia. The authors have been developing implantable probe to observe microcirculation in the experimental animal. As mentioned above, it is gradually improving at the points of size, magnification and focus mechanism. Magnification and probe size were almost satisfactory to be implanted. Residual problems are to develop a micro focus mechanism and illumination. Our final goal is to observe not only thin and soft tissue like a connective tissue but also to observe organ circulation such as heart, kidney, etc. For that purpose, it would be important to clarify what kind of light(wave length, brightness, transmission or reflect, etc) should be projected..

References

1. K. Imachi, T. Chinzei, Y. Abe, T. Isoyama, K. Mabuchi, K .Imanishi, T. Ono, A. Kouno, M. Kusakabe, K. Atsumi and I. Fujimasa: A new apparatus for chronic observation of microcirculation in-situ to evaluate an artificial organ performance. ASAIO Journal, 40(3) M757-761, 1994
2. K. Imachi, Y.Abe, T.Chinzei, K.Mabuchi, K.Imanishi, T.Isoyama, A.Kouno, T.ono and I.Fujimasa: Factors Influencing hemodynamics blood chemical data and hormone socretion of total artificial heart goat. In Progress in Microcirculation Research(H. Niimi, M. Oda, T. Sawada, R-J Xiu ed), Pergamon Press, London, 453-458, 1994
3. K. Imachi, T. Chinzei, Y. Abe, T. Isoyama, K. Mabuchi, K. Imanishi, T. Ono, A. Kouno, M. Kusakabe, M. Onuma, K. Atsumi and I. Fujimasa: Development of a new apparatus to observe the microcirculation chronically in a continuous flow blood pump research. Artificial Organs, 19(7), 723-728,1995
4. K. Imachi, T. Chinzei, Y. Abe, T. Isoyama, K. Mabuchi, K. Imanishi, M. Kusakabe, M. Ohnuma, and I. Fujimasa: A new method for the chronic evaluation of the microcirculation during artificial heart pumping. In Heart Replacement-Artificial Heart 5(T. Akutsu, H. Koyanagi ed), Springer-Verlag, Tokyo, 281-287, 1996

Address of the corresponding author

Kou Imachi
Tohoku University, TUBERO
2-1 Seiryo-machi, A0ba
Sendai, Japan
imachi@tubero.tohoku.ac.jp

IFMBE Proceedings Volume 14, 2006
World Congress on Medical Physics and Biomedical Engineering (ISBN: 3-540-36839-6)

In vivo measurements and constitutive modeling of colon tissue

M. Higa[1], Y. Luo[1], T. Okuyama[2], Y. Shiraishi[3], H. Liu[3], T. Yambe[3] and T. Takagi[2]

[1] Biomedical Engineering Research Organization, Tohoku University, Sendai, Japan
[2] Institute of Fluid Science, Tohoku University, Sendai, Japan
[3] Institute Developing Aging and Cancer, Tohoku University, Sendai, Japan

Abstract— **This study aims at measuring the mechanical properties of the colon and developing a constitutive model of them. For this, in vivo compression experiments on the colon of a goat were performed by measuring force-displacement relations and time dependent stress relaxation data under general anesthesia. Force-displacement data were converted to stress-strain data using tissue thickness measured by a laser displacement meter. Compression tests of this study have two phases; a compression phase under three constant compression rates and a stress relaxation phase under constant strain after compression. In this study, viscoelastic parameters were decided at first from the stress relaxation curves, and then nonlinear parameters were decided considering viscoelasticity. In stress relaxation phase, a reduced-stress relaxation function and generalized Maxwell model were applied to express the constitutive model of tissues that have viscoelastic behaviors. Parameters of this model were computed by fitting the constitutive model to the experimental results of stress relaxation. The constitutive model with calculated parameters have shown good agreement with experimental data. Then nonlinear parameters of stress-strain relation were computed. In the compression phase, results revealed highly nonlinear force-displacement behavior and strong dependence on compression rates. In this study, Mooney-Rivlin model incorporated convolution integral of viscoelastic constitutive model that has calculated parameters of relaxation phase was applied. Every nonlinear parameter was computed by fitting the constitutive model to the experimental results during compression phase.**

Keywords— **colon tissue, mechanical properties, mathematical modeling, nonlinear, viscoelasticity**

I. Introduction

Recent years, various artificial internal organs and computer-aided surgery have been available. Going with these developing, the accurate measurement of mechanical properties of living bodies are of basic subject in biomechanics and immerse technological importance to apply these technique in clinical field. Many researchers have examined the mechanical properties of soft tissues and some reports regarding the colon have been published [1]-[4]. However, most reports about the colon have been based on tensile examinations, in which samples that had been surgically excised from animals or humans were pulled on a tensiometer. The mechanical properties of soft tissues in these in vitro examinations may show different values from that are measured in vivo [5].

The objective of the present study is to determine the passive mechanical properties of colon. The authors have been developing artificial internal organs implanted beside the colon and precise information of mechanical properties is of a great interest. To measure small force and large deformation in vivo, an original force-displacement acquisition machine developed by the authors was used. Parameters of constitutive models considering nonlinear and viscoelasticity of tissue were determined.

II. Compression experiments of goat in vivo

Experimental set-up

Compression experiments aims at estimating the constitutive relation of colon tissue. An adult nanny-Saanen goat

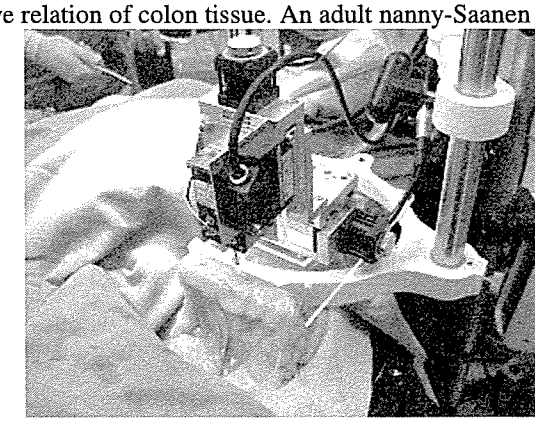

Fig.1 Experimental setting of in vivo compression

was used in this experiment. After intramuscular administration of atropine sulfate, anesthesia was induced via an endotracheal tube. Anesthesia was maintained throughout the experiment with 2.5% halothane. The respiration rate was fixed at 15 min^{-1} by a ventilator. Following laparotomy, the pancuronium bromide was injected into the jugular veins in order to abolish contractile activity in the gastroin-

testinal tract. After obtaining muscle relaxation, a part of the descending colon was bilaterally exposed by celiotomy. The proximal part from the arteria mesenterica caudalis was used as an experimental sample. The residual contents in the lumen were gently cleared using physiological saline. Special care was taken to maintain the viability of the tissue during experiments by preserving the neurovascular supply for the large intestine. Fig.1 shows the experimental setting scene when ready to start experiments.

Experimental procedures and data acquisition

The testing apparatus consists of a one-dimensional linear stage (QT-CD1, Chuo Precision Industrial Co., LTD.) and a load cell (UT-500GR, rated capacity=4.9 N, MINEBEA Co., LTD.). The tissue thicknesses were measured by a laser displacement meter (LB-60, KEYENCE, Co., LTD.) before every test. Compression velocities of 0.02, 0.5, 5 mm/s were applied. The tissue was compressed until 0.2 mm thickness in each velocity, and then maintained 0.2 mm thickness for 300 seconds. The loading positions on the tissue were changed in each test and no preconditioning was carried out.

The stress *(S)* was computed from the cross-sectional area *(A)* of the compression platen and the force *(F)* as:

$$S=F/A \tag{1}$$

Fig.2 shows calculated stress versus strain. Time zero represents the moment to start compression.

To model the stress relaxation, recorded force value was normalized to produce reduced-stress relaxation function *E(t)* is denoted as:

$$E(t)=S(t)/S_{max} \tag{2}$$

where *S(t)* is the stress calculated from equation (1) and S_{max} is the stress value at *t=0* (*S(0)*). Fig.3 shows time versus *E(t)*. Time zero represents the moment to stop loading. Tests were carried out three times in each velocity by changing compress positions. Data were averaged in each compression rate to calculate the stress.

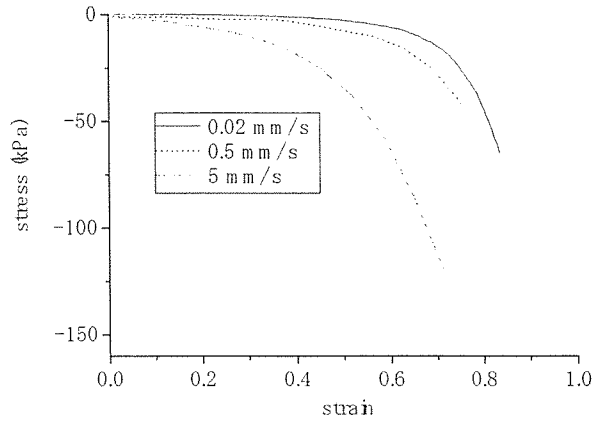

Fig. 2 Sress versus strain curve during compression phase

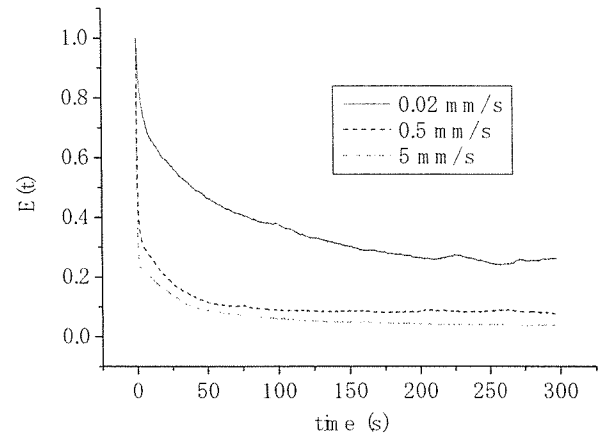

Fig.3 Stress versus time curves during relaxation phase

III. Constitutive Model of the Colon

Compression experiments itself provide only force-displacement and force-time data. In this section, we choice for a constitutive law and decide each parameter value of the low using the stress-strain and stress-time data derived from equation (1) and (2).

To begin the modeling of non-linear stress-strain dependence, the strain energy function of the following form is used:

$$W=\sum_{i+j=1}^{n} a_{ij}(J_1-3)^i(J_2-3)^j \tag{3}$$

where the strain invariants J_i are:

$$J_1 = \lambda_1^2 + \lambda_2^2 + \lambda_3^2$$
$$J_2 = \lambda_1^2\lambda_2^2 + \lambda_2^2\lambda_3^2 + \lambda_3^2\lambda_1^2 \quad (4)$$
$$J_3 = \lambda_1\lambda_2\lambda_3 = 1$$

where λ_i are stretch ratio. Here, the tissue is assumed to be isotropic, homogeneous and incompressible. The first two terms of equation (3) namely Mooney-Rivlin model [6] was adopted in this study same as other studies of mathematical modeling of soft tissue [5] [7].

To model the mathematical expression of *E(t)* in equation (2), Generalized Maxwell model was used:

$$E(t) = E_\infty + \sum_{i=1}^{n} E_i \exp(-t/\tau_i) \quad (5)$$

where E_∞, n, E_i and τ_i are final elastic modulus, the number of Maxwell elements, elastic modulus at *ith* element, and relaxation time at *ith* element respectively. In this study, two elements of Prony series (n=2) were used because the relaxation curve showed that at least two phase of relaxation were apparent. Although more number of series would be able to express the experimental results more precisely, the number of elements was limited to two for simple calculation. To obtain a good agreement between the theory and experimental result expressed in Fig.2. *E(t)* was normalized by initial elastic modulus E_0 then $n=2$ is substituted into equation (5):

$$g(t) = E(t)/E_0 = (1 - g_1 - g_2) + g_1 \exp(-t/\tau_1) + g_2 \exp(-t/\tau_2)$$
$$(0 < g(t) \le 1, g(0) = 1) \quad (6)$$

In this study, the result in the fastest velocity of stress relaxation (5 mm/s) was used to fit the equation (6) because other results in slow velocity did not showed two-phase stress relaxation clearly. First phase of stress relaxation seems to have completed during compression in these slow velocity. Fig. 4 shows the experimental data and fitting curve. Coefficient of correlation R^2 was 0.9916. Obtained parameters are listed in table 1.

In the next step, non-linear parameters a_{0l}, a_{l0} are calculated using parameters of *g(t)* calculated before. To model the time-dependent nonlinear behavior of the tissue, the energy function can be written in the form of a convolution integral considering equation (3) and (6):

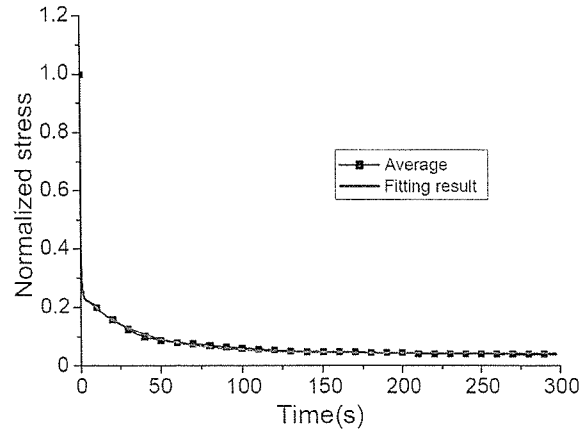

Fig. 4 Experimental data and constitutive model curve fitting during stress relaxation phase. Coefficient of correlation (R^2) was 0.9916

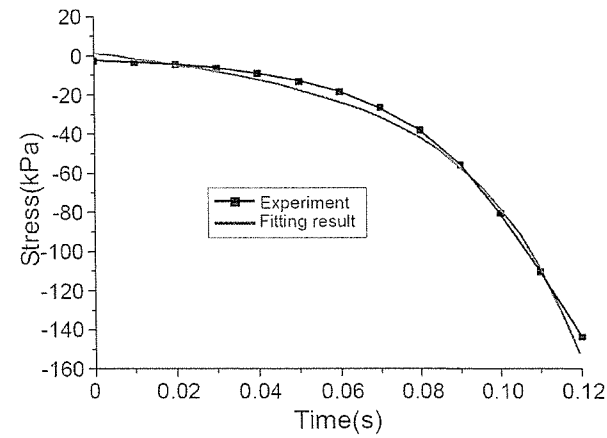

Fig. 5 Experimental data and constitutive model curve fitting during compression phase. Coefficient of correlation (R^2) was 0.9930.

$$W = \int_0 \sum_{i+j=1}^{n} g(t-s)\frac{d}{ds}\left[a_{ij}(J_1 - 3)^i (J_2 - 3)^j\right] ds \quad (7)$$

where integral variable s represents a infinitesimal time within time 0 to t. Stress value can be written in following simple differentiation.

$$S(t) = \frac{\partial W}{\partial \lambda} \quad (8)$$

To calculate such equation, $\lambda = 1 + vt$ (v=compression velocity) was substituted into equation (7). Fig.5 shows the experimental data and fitting curve during compression phase. The fastest velocity (v=5 mm/s) was also used in this fitting.

Calculated parameters were also listed in table1. Coefficient of correlation R^2 was 0.9930.

Table 1 Calculated parameters and coefficient of correlations

Parameter	Value	R^2
g_1	0.75	0.9916
g_2	0.20	
τ_1	0.23 s	
τ_2	35 s	
a_{10}	7.5 kPa	0.9930
a_{01}	-0.79 kPa	

IV. Discussion

An in vivo measurement of passive mechanical properties of the colon in the goat is described. This measurement is a first report that assesses the nonlinear mechanical properties considering viscoelasticity of the colon. According to the results of in vivo compression, the colon tissues exhibit nonlinear stress-strain relation as well as strong dependence on strain rate. As a result of stress relaxation, two phases of stress relaxations were observed at least and the first relaxation time τ_1 is very quick that could not be observed with slow compression rate.

The use of Mooney-Rivlin model with time-dependent coefficients, written in the form of convolution integral of two elements of Hyper-viscoelastic model required six parameters. These constitutive equations adopted in this study and obtained six parameters listed in table 1 enable us to perform the three-dimensional finite element (FE) modelling of the colon. As a result, stress distribution in the colon is calculable when external load was applied to the tissue as well as feed back force value when laparoscopic-assisted robotic surgery.

Acknowledgement

The authors are grateful to the financial support of Special Coordination Funds for Promoting Science and Technology from the Ministry of Education, Culture, Sports, Science and technology.

All animals used in experiments were cared for in strict compliance with Research Animal Resource Committee Guideline of the Institute of Experimental Animals, Tohoku University School of Medicine.

References

1. Egorov, V. I., Schastlivtsev, I. V. et al. (2002) Mechanical properties of the human gastrointestinal tract. J. Biomechanics 35:1417–1425
2. Gao, C. et al. (2000) Biomechanical and morphological properties in rat large intestine. J. Biomechanics 33:1089-1097
3. Watters, D.A. et al. (1985) Mechanical properties of the rat colon: the effect of age, sex and different conditions of storage. Quarterly Journal of Experimental Physiology 70 (1): 151-162
4. Yamada, H., Strength of Biological Materials, 2nd edition. 1972; Williams and Watkins, Baltimore.
5. Millar, K. et al. (2000) Mechanical properties of brain tissue *in vivo*: experiment and computer simulation. J. Biomechanics 33: 1369-1376
6. M. Mooney (1940) A theory of large elastic deformation. J. Applied Physics 11, Sep.: 582-592
7. Millar, K. and Chinzei K (1997) Constitutive modeling of brain tissue: experiment and theory. J. Biomechanics 30:1115-1121

Address of the corresponding author:

Author: Masaru Higa
Institute: Tohoku University Biomedical Engineering Research Organization
Street: Aoba-ku Seiryo 2-1
City: Sendai
Country: Japan
Email: masaru@tubero.tohoku.ac.jp

SICE-ICASE International Joint Conference 2006
Oct. 18-21, 2006 in Bexco, Busan, Korea

Autonomic Nervous Activity Revealed by a New Physiological Index ρ_{max} Based on Cross-Correlation between Mayer-Wave Components of Blood Pressure and Heart Rate

Akira Tanaka[1], Norihiro Sugita[2], Makoto Yoshizawa[3], Yasuyuki Shiraishi[4],
Tomoyuki Yambe[4] and Shin-Ichi Nitta[4]

[1] Faculty of Symbiotic Systems Science, Fukushima University, Fukushima, Japan
(Tel : +81-24-548-8411; E-mail: a-tanaka@sss.fuskuhima-u.ac.jp)
[2] Graduate School of Engineering, Tohoku University, Sendai, Japan
(Tel : +81-22-795-7130; E-mail: sugita@yoshizawa.ecei.tohoku.ac.jp)
[3] Information Synergy Center, Tohoku University, Sendai, Japan
[4] Institute of Development, Aging and Cancer, Tohoku University, Sendai, Japan

Abstract: The authors have proposed a new physiological index ρ_{max} which is the maximum cross-correlation coefficient between blood pressure and heart rate whose frequency components are limited to the Mayer wave-band (0.04-0.15Hz). The advantages of this index are small individual difference and high reproducibility compared with other physiological indices which are calculated independently single cardiovascular measurements. The previous study showed that the index ρ_{max} is possible to assess visually-induced motion sickness. However, the relation between the proposed index and autonomic nervous activity has not been clarified yet. In this study, the change in ρ_{max} during sympathetic or parasympathetic blockage has been investigated in comparison with conventional indices in an animal experiment. The results have indicated that ρ_{max} does not have information on parasympathetic nerve activity but sympathetic one.

Keywords: heart rate, blood pressure, autonomic nerve function.

1. INTRODUCTION

In order to assess the biological effect of visual stimulation in terms of autonomic nervous activity, the authors have proposed a new physiological index ρ_{max} which is the maximum cross-correlation coefficient between blood pressure and heart rate whose frequency components are limited to the so-called Mayer wave-band (0.04-0.15Hz). The reason why only Mayer waves (10s period or 0.1Hz components; LF component) included in blood pressure and heart rate were used is the relationship between them can reflect the difference between the resting state and the exiting state caused by visual stimulation. The advantages of this index are small individual difference and high reproducibility compared with other physiological indices which are calculated independently from cardiovascular measurements [1]. Therefore the authors have introduced ρ_{max} for evaluation of the effect of visual stimulation. The previous study showed that the physiological index ρ_{max} is possible to assess visually-induced motion sickness more apparently than conventional indices such as the LF/HF of heart rate [1]-[3]. However, the relation between the proposed index and autonomic nervous activity has not been clarified yet. In this study, the change in ρ_{max} during sympathetic or parasympathetic blockage has been investigated and compared with conventional indices in an animal experiment.

2. METHODS

The proposed physiological index ρ_{max} was calculated as the following steps.

First, the beat-to-beat variables, heart rate HR [min^{-1}] and mean blood pressure MBP [mmHg], were interpolated by the cubic spline function to be time-continuous functions, and they were re-sampled every ΔT=0.2s. After that, each data was filtered through a band-pass filter with a bandwidth between 0.04Hz and 0.15Hz to extract the Mayer wave components.

Let k denotes the discrete time based on $t = k\Delta T$. For simple expression, let $x(k) = -MBP(k)$ and $y(k) = HR(k)$. The minus sign shown in $-MBP$ was introduced so that $x(k)$ and $y(k)$ might become as in-phase as possible for simple interpretation in depicted figures. The cross-correlation coefficient ($\rho_{xy}(\tau)$; the cross-correlation function normalized by root mean square values of input and output signals at lag time $\tau = k\Delta T$) from $x(k)$ to $y(k)$ was calculated time-discretely on the basis of 2min data (600samples) segmented by the Tukey window as follows:

$$\rho_{xy}(\tau) = \frac{\phi_{xy}(\tau)}{\sqrt{\phi_{xx}(0) \cdot \phi_{yy}(0)}} \qquad (1)$$

where $\phi_{xx}(\tau)$ and $\phi_{yy}(\tau)$ are auto-correlation functions of $x(t)$ and $y(t)$, respectively, and $\phi_{xy}(\tau)$ is the cross-correlation function from $x(t)$ to $y(t)$. The maximum value of lag time τ was 10s (50samples). Furthermore, the maximum cross-correlation ρ_{max}, i.e. the maximum value of $\rho_{xy}(\tau)$ for the positive τ, was obtained as

$$\rho_{max} = \max_{0s<\tau<10s} \rho_{xy}(\tau) \qquad (2)$$

89-950038-5-5 98560/06/$10

3. EXPERIMENT

The goat used in the experiment weighted 50kg. The goat was anesthetized by halothane inhalation. After tracheal tube intubation by tracheotomy, the distal end was connected to a respirator. Electrodes for the electrocardiodiagram (ECG) were attached to the legs. Arterial blood pressure *BP* was measured with a catheter inserted into the artery through the left femoral artery. ECG and *BP* ware stored in a personal computer every 1ms.

After the control data was stored, atropine was injected in order to block parasympathetic nerve activity. Then propranolol was injected after physiological parameters returned to the same level as the control level.

HR was calculated from the reciprocal of the inter-R-wave interval of the ECG signal. *MBP* was obtained as the mean value of the pressure signal over one heartbeat.

CVRR, %RR50 which are known as the indices of parasympathetic nerve activity were calculated for each dataset which was segmented into 2min (600samples) 5min after infusion. %RR50 is defined as the percentage of normal R-R intervals that changed in absolute value by more than 50 msec from the previous interval. The CVRR is defined as the ratio of the standard deviation of the R-R intervals to their average value.

ρ_{max} was calculated time-discretely on the basis of 2min-long data segmented by the Hamming window from -1min to 1min.

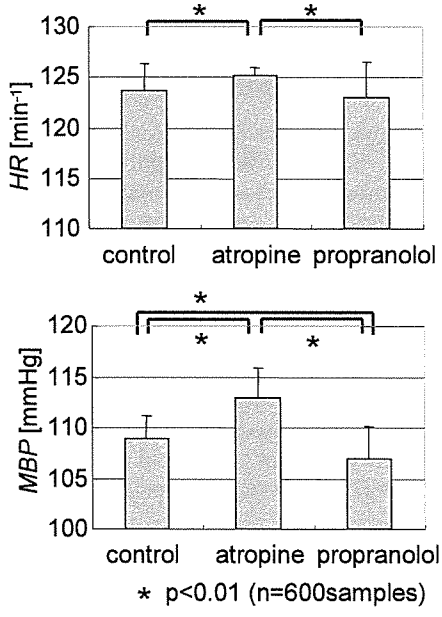

Fig. 1 Difference in physiological parameters within each condition.

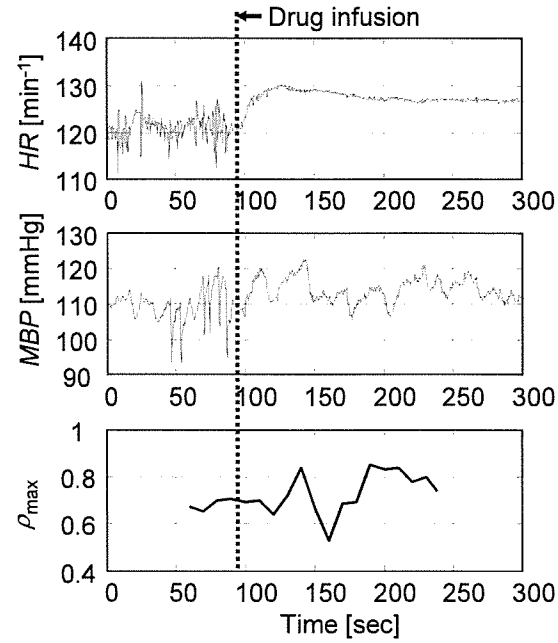

Fig. 2 Change in *HR*, *MBP and* ρ_{max} after atropine infusions.

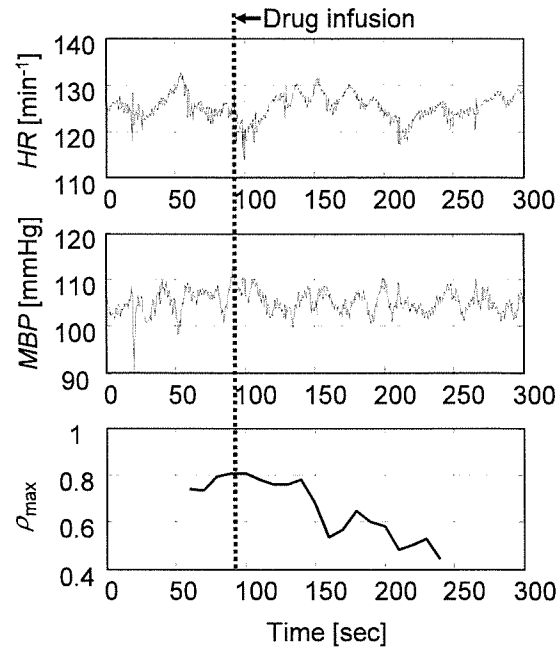

Fig. 3 Change in *HR*, *MBP* and ρ_{max} after propranolol infusions.

4. RESULT

Fig. 1 shows the changes in *HR* and *MBP* caused by drug infusions. *HR* and *MBP* increased significantly in atropine injection. On the other hand, *MBP* decreased

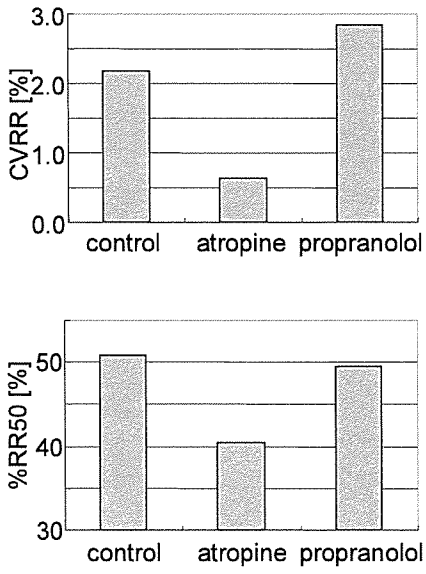

Fig. 4 Change in CVRR and %RR50 Difference in physiological parameters within each condition.

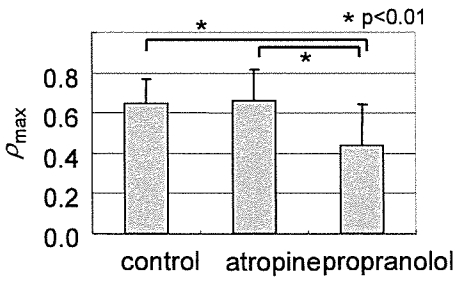

Fig. 5 Change in ρ_{max} after drug infusions.

significantly in propranolol injection. Fig. 2 and 3 show the transient response of *HR*, *MBP* and ρ_{max} to atropine and propranolol infusion, respectively. Atropine infusion makes *HR* increase and fluctuation of *HR* decrease. In atropine infusion, there is no specific tendency in ρ_{max}. On the other hand, it can be seen that ρ_{max} decreases after propranolol infusion.

Fig. 4 shows CVRR and %RR50 of each dataset segmented into 2min 5min after the drug infusions. CVRR and %RR50 decreased in atropine injection.

Fig. 5 shows the change in ρ_{max} after drug infusions. ρ_{max} significantly decreased in propranolol injection though there is no significant change in atropine injection.

5. DISCUSTION

The parasympathetic blockage caused decrease of CVRR and %RR50 which are known as the indices of parasympathetic nerve activity though there was no significant change in ρ_{max}. On the other hand, the sympathetic nerve blockage caused marked decrease in ρ_{max}. These results indicate that ρ_{max} represents the sympathetic nerve activity. In the authors' previous study, ρ_{max} and the LF/HF had different changes during visual stimulation though the LF/HF also represents sympathetic nerve activity. This seems to be because ρ_{max} includes the information on cardiovascular regulation via not only heart rate variability but also vascular regulation. Thus, it seems that vascular regulation mainly contributes to the change in ρ_{max} for physiological and/or psychological stimuli such as visual stimulation.

To clarify the effect of each of heart rate and vascular regulations upon ρ_{max}, the closed-loop identification using AR model [4] may be effective as well as the tifurther experiment using drugs which preferentially affect vascular regulation such as alpha blockers.

6. CONCLUSIONS

In this study, the basic characteristics of ρ_{max} previously proposed by the authors ha ve been investigated by an animal experiment. It was shown that ρ_{max} is associated with the sympathetic nervous function.

Actually, the baroreflex system has multivariable feedback loops. However, analysis of ρ_{max} is based on the hypothesis that the system can be regarded as a single-input and single-output open-loop system. In further studies [5], therefore, we should compare the results of ρ_{max} with causal coherency functions used by Porta [6]. The causal coherency functions can divide linearity of the baroreflex system into two independent parts of linearity, i.e., the baroreflex arch and mechanical arch.

In further studies, it is necessary to evaluate the effect of each of heart rate and vascular regulations upon ρ_{max}.

REFERENCES

[1] N. Sugita, M. Yoshizawa, A. Tanaka, K. Abe, T. Yambe, S. Nitta, "Evaluation of effect of visual stimulation on humans based on maximum cross-correlation coefficient between blood pressure and heart rate (in Japanese)," *J. Human Interface Society of Japan*, vol.4, No. 4, pp. 39-4 6, 2002.

[2] T. Shioiri, M. Kojima, T. Hosoki, H. Kitamura, A. Tanaka, T. Bando, T. Someya, "Momentary changes in the cardiovascular autonomic system during mental loading in patients with panic disorder: a new physiological index "rho(max)"," *J Affect Disord*, vol. 82, No. 3, pp. 395-401, 20 04.

[3] N. Sugita, M. Yoshizawa, A. Tanaka, K. Abe, T. Yambe, S. Nitta, S. Chiba, "Biphasic Response of Autonomic Nervous System to Visually-Induced Motion Sickness (in Japanese)," *Trans. of the Virtual Reality Society of Japan*, vol. 9, No. 4, p p. 369-375, 2004.

[4] G. Baselli, A. Porta, O. Rimoldi, M. Pagani, S. Cerutti, "Spectral decomposition in multichannel